RAA 2015 Vol. **15** No. **10**, 1725–1734 doi: 10.1088/1674–4527/15/10/009
http://www.raa-journal.org *http://www.iop.org/journals/raa*

Research in Astronomy and Astrophysics

Fine-scale structures and material flows of quiescent filaments observed by the New Vacuum Solar Telescope

Xiao-Li Yan[1,2], Zhi-Ke Xue[1], Yong-Yuan Xiang[1] and Li-Heng Yang[1]

[1] Yunnan Observatories, Chinese Academy of Sciences, Kunming 650011, China; *yanxl@ynao.ac.cn*
[2] Key Laboratory of Solar Activity, National Astronomical Observatories, Chinese Academy of Sciences, Beijing 100012, China

Received 2014 July 18; accepted 2015 February 12

Abstract Study of the small-scale structures and material flows associated with solar quiescent filaments is very important for understanding the formation and equilibrium of solar filaments. Using high resolution Hα data observed by the New Vacuum Solar Telescope, we present the structures of barbs and material flows along the threads across the spine in two quiescent filaments on 2013 September 29 and on 2012 November 2, respectively. During the evolution of the filament barb, several parallel tube-shaped structures formed and the width of the structures ranged from about 2.3 Mm to 3.3 Mm. The parallel tube-shaped structures merged together accompanied by material flows from the spine to the barb. Moreover, the boundary between the barb and surrounding atmosphere was very neat. The counter-streaming flows were not found to appear alternately in the adjacent threads of the filament. However, the large-scale patchy counter-streaming flows were detected in the filament. The flows in one patch of the filament have the same direction but flows in the adjacent patch have opposite direction. The patches of two opposite flows with a size of about $10''$ were alternately exhibited along the spine of the filament. The velocity of these material flows ranged from 5.6 km s^{-1} to 15.0 km s^{-1}. The material flows along the threads of the filament did not change their direction for about two hours and fourteen minutes during the evolution of the filament. Our results confirm that the large-scale counter-streaming flows with a certain width along the threads of solar filaments exist and are coaligned well with the threads.

Key words: Sun: filaments, prominences — Sun: activity — Sun: corona

1 INTRODUCTION

Solar prominences/filaments are relatively cool and high density structures that are embedded in the chromosphere and the million-degree corona (Hirayama 1985; Tandberg-Hanssen 1995). Prominences appear as bright structures against the dark background above the solar limb. When projected on the solar disk, they exhibit darker structures than their surroundings in chromospheric lines.

Filaments are typically long-lived features, ranging from about one day to several weeks. Filaments exhibit many characteristics that are different from sunspots in a solar cycle (Li et al. 2010; Kong et al. 2014, 2015). In general, quiescent filaments have two linked categories of structures: "spines" and "barbs." A "spine" is the highest part of a quiescent prominence that forms an axis that is horizontal and is composed of many resolvable threads, while "barbs" are connected to the spine and terminate in the chromosphere (Martin 1998). Moreover, the filament threads in quiescent filaments are shorter than those in active region filaments (Zhou et al. 2014).

The counter-streaming flows along closely spaced vertical regions of a prominence between its top and the lower solar atmosphere were reported by Zirker et al. (1998). It has been well-established observationally that the entire filament bodies are composed of numerous thin threads, which are largely horizontal and oriented at angles of 20–25 degrees relative to the long axis of the filament (Engvold et al. 2001). The filament threads may represent separate flux tubes (Engvold 1998). Lin et al. (2003) found that the net velocities of the counter-streaming flows in the two directions are about 8 km s^{-1}. The width of the thin threads is $\leq 0.3''$, and the velocity of the continuous flow along the threads is about 15 km s^{-1} (Lin et al. 2005). A small-amplitude wave propagates along a number of filament threads with an average phase velocity of 12 km s^{-1} and a wavelength of $4''$, and the oscillatory period of individual threads varies from 3 to 9 minutes (Lin et al. 2007). By using the off-band Hα observation of Hida/DST, Schmieder et al. (2008) reported that the counter-streaming flows in the filament were detected before its eruption and its velocity was 10 km s^{-1}. The merger, separation and oscillation of the filament spines were found by Ning et al. (2009a). Cao et al. (2010) found that the upflows at the filament footpoint were driven by the oscillation of the solar surface. The dip model of prominences claims that the barb is supported by means of a dip in the magnetic field lines over the minor polarity (Aulanier & Demoulin 1998; van Ballegooijen 2004). Chae et al. (2005) found that the terminating points of the barbs occurred above the minor polarity inversion line by comparing the Hα images with magnetograms taken by SOHO/MDI and the flux cancellation proceeded on the polarity inversion line. Their results are in accordance with the idea that filament barbs are cool plasma suspended in the local dips of the magnetic field lines formed by magnetic reconnection in the chromosphere. The formation and disappearance of filament barbs may be connected with the flows (Joshi et al. 2013). The emergence and cancellation of magnetic flux may also cause the formation or disappearance of the magnetic structures of the barb (Li & Zhang 2013). The larger-scale patchy counter-streaming flow in EUV along the filament channel from one polarity to the other observed by Hinode/EIS was found to be related to the intensity of a plage or active network (Chen et al. 2014).

Up to now, there have been two viewpoints on the counter-streaming flows: one relies on steady bidirectional streaming everywhere in the filament along adjacent closely spaced threads (Zirker et al. 1998); the other considers larger-scale patchy counter-streaming flows in EUV along the filament channel from one polarity to the other (Chen et al. 2014). Chen et al. (2014) have found no EUV counterpart of the fine-structured Hα counter-streaming flow along the filament channel, as implied by Zirker et al. (1998). They explained that the ubiquitous Hα counter-streaming flows found by previous researchers are mainly due to longitudinal oscillations of filament threads, which are not in phase with each other. The larger-scale patchy counter-streaming flows are another component of unidirectional flows inside each filament thread in addition to the longitudinal oscillation. Therefore, the nature of the material flows in the filament threads deserves further investigation. In addition, although the structures of quiescent filaments have also been studied for decades, the fine-scale structures of filament barbs and spines are still essentially unclear at present. To address these issues, we present two quiescent filaments observed by the New Vacuum Solar Telescope (NVST) to show small-scale structures and the evolution of filament barbs and the material flows in the filament threads.

Section 2 gives observation and data processing. Results are described in Section 3. Conclusion and discussion are shown in Section 4.

2 OBSERVATION AND DATA PROCESSING

The NVST is a vacuum solar telescope with a 985 mm clear aperture. The vacuum system consists of two vacuum tubes because the telescope should rotate on its altitude axis in addition to its azimuth axis. These two vacuum tubes are separated by two vacuum windows. An optical window (W1) with a diameter of 1.2 meters is placed on the top of the vacuum tube to keep the air pressure inside the tube lower than 70 Pa. The optical system after W1 is a modified Gregorian system with an effective focal length of 45 m. The primary mirror is a parabolic imaging mirror with a clear aperture of 985 mm. Detailed information about NVST can be referenced in Liu et al. (2014). The NVST is one of the primary observational facilities at the Fuxian Solar Observatory (FSO). The other two facilities are the Optical and Near-infrared Solar Eruption Tracer (ONSET) (Fang et al. 2013) and the new digital spectrometer (Gao et al. 2014). The main scientific goal of NVST is to observe fine-scale structures in both the photosphere and chromosphere. A multi-channel high resolution imaging system was set up and one chromospheric channel and two photospheric channels can now be used to acquire observations (Wang et al. 2013). The tracking accuracy of NVST is less than $0.3''$. The Hα filter is a tunable Lyot filter with a bandwidth of 0.25 Å. Thanks to the good atmospheric seeing of Fuxian lake, observations at NVST can last for several hours. The data used in this study were obtained by the NVST in Hα 6562.8 Å from 00:51:12 UT to 04:12:08 UT on 2013 September 29 and from 05:53:07 UT to 08:07:56 UT on 2012 November 2. The cadence of Hα observations is 12 s and the pixel size is $0.16''$. The reduced data from NVST are classified into two levels. One is the Level 1 data that are processed by frame selection (lucky imaging) (Tubbs 2004). The other is Level 1+ data that are reconstructed by speckle masking (Weigelt 1977; Lohmann et al. 1983) or iterative shift & add (ISA; Liu et al. 1998). The Hα data used in this paper were dark current subtracted and the flat field was corrected to Level 1, and then the Level 1 data were reconstructed to Level 1+ with the speckle masking method of Weigelt (1977). The images were co-aligned by using the subpixel registration algorithm (Feng et al. 2012; Yang et al. 2014).

3 RESULTS

Figure 1 shows the high-resolution Hα image of the quiescent filament observed by NVST at 00:51:12 UT on 2013 September 29. The quiescent filament was located in the northwest part of the Sun. The center of the field of view was located at $x = 240''$ and $y = 450''$. Due to the field of view, only a part of the quiescent filament was observed. The quiescent filament was very mature and large with a large barb and spine. This filament started to appear on the east part of the Sun on 2013 September 20, which was found by checking Hα data from Big Bear Solar Observatory. The threads of the barb smoothly transited into the spine. Moreover, the boundary between the barb and the outer atmosphere was very neat. To address the special structures of the barb, we measured the intensity of the barb and the outside atmosphere. The difference in the intensity between both sides of the boundary of the barb is about 10%. This illustrates that each side of the boundary has different magnetic structures. Up to now, we have not found why the boundary between the barb and the outer atmosphere is so obvious. We conjecture that this structure may be related to the special magnetic structures of the barb. When quiescent filaments appear at the solar limb, the bright arched structures are often observed (see fig. 3b and 3c in Mackay et al. 2010). Many vertical threads appear connecting the boundary of the arched structures with the spine of the prominences. Moreover, there is a cavity below the arched magnetic structure. We suspect that the obvious boundary between the barb and the outside may be due to the projection of the arched structures of the quiescent filaments on the Sun. Confirmation of this speculation needs continuous high resolution observations to trace the evolution of solar filaments from the solar disk to the limb.

Figure 2 shows the evolution of the barb from 01:20:52 UT to 04:09:23 UT. At the beginning, the barb is composed of parallel narrow threads, similar to those in the spine. The individual threads gradually blend with the neighboring threads. After half an hour, the intensive narrow threads

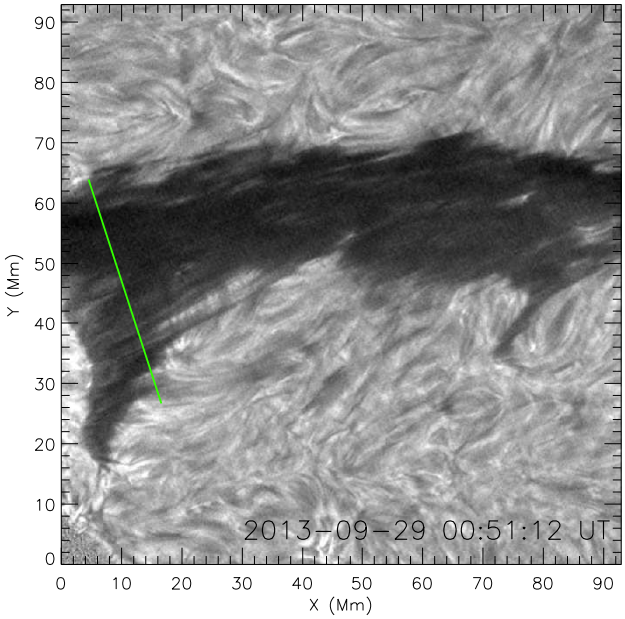

Fig. 1 High-resolution Hα image of the quiescent filament observed by NVST at 00:51:12 UT on 2013 September 29. The green line is used to mark the position of the time slice shown in Figure 3.

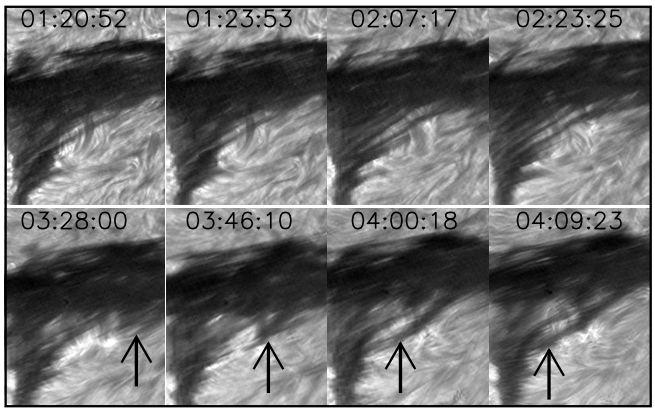

Fig. 2 Sequence of high-resolution Hα images that show the evolution of the filament barb from 01:20:52 UT to 04:09:23 UT on 2013 September 29. The black arrows indicate the materials, which are flowing from the spine to the barb.

evolved into the distinct parallel tube-shaped structures. The structures were maintained for about half an hour and began to merge together, accompanied by the material flow from the spine to the barb. The black arrows in Figure 2 indicate material flows from the spine to the barb. The typical width of the threads in the quiescent filaments is between $0.2''$ and $0.3''$ (Lin et al. 2005). The pixel size of Hα in the Level 1+ data is $0.16''$. The resolution of NVST can identify the threads of the quiescent filament. The width of the parallel tube-shaped structures was larger than the typical size of

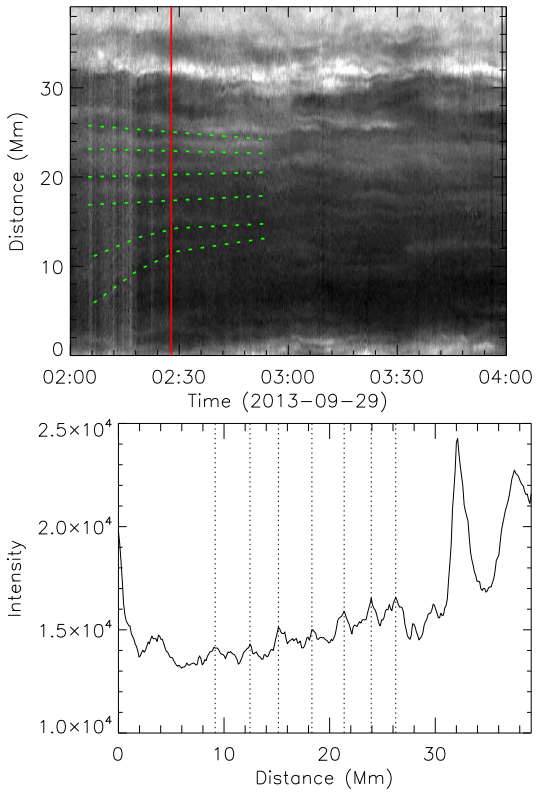

Fig. 3 *Upper panel*: A time slice taken from high-resolution Hα images at the position marked by the green line in Fig. 1. The green dotted lines indicate the six parallel flux tube-shaped structures formed in the barb. *Lower panel*: The intensity along the red line in the upper panel. The vertical dotted lines outline the widths of the six tube-shaped structures that were formed during the evolution of the barb.

individual threads. This evolution process of the filament can be seen from supplementary movie 1 (*http://www.raa-journal.org/docs/Supp/ms1934movie1.avi*).

In order to show the change in the barb, we make a time slice along the green line in Figure 1. The time slice is shown in the upper panel of Figure 3. The length of the slice is 40 Mm and the time is from 02:00 UT to 04:12 UT. The green dotted lines indicate the six parallel flux tube-shaped structures that formed in the barb. The six parallel tube-shaped structures had a converging motion and gradually merged with each other. The change in intensity along the red line in the upper panel of Figure 3 can be seen from the lower panel of Figure 3. The vertical dotted lines are marked to show the widths of the six parallel tube-shaped structures. The widths of the structures are 3.3, 2.7, 3.2, 3.1, 2.6 and 2.3 Mm. The average width is about 2.9 Mm. The plasma flowing along the filament threads may be considered as evidence for the alignment of threads along the local magnetic field. This scenario is suitable for flows in the horizontal magnetic fields of the quiescent filament. However, the flows in the vertical structures of the quiescent filaments may not be aligned with the field because the velocities of the flows in the vertical threads of the quiescent filaments are lower than their free-fall velocities. Chae et al. (2008) explained the vertical threads of the quiescent prominence in terms of magnetic dips in the initially horizontal magnetic fields. To our knowledge,

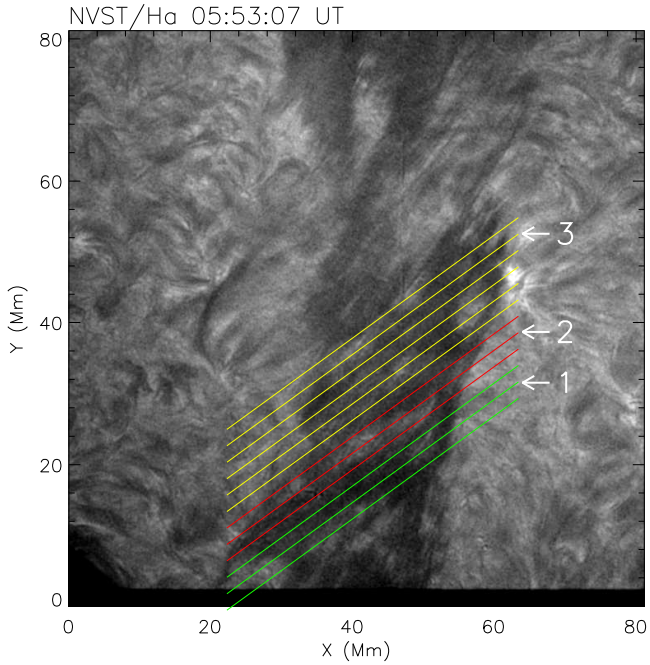

Fig. 4 High-resolution Hα image of the quiescent filament observed by NVST at 05:53:07 UT on 2012 November 2. The green and yellow lines mark the areas that have material flows with the same direction and the red lines denote material flows in opposite directions. The lines marked by the numbers indicate the positions of the time slices shown in Fig. 5.

the formation of the tube-shaped structures in a regular arrangement during the evolution of the barb has not been reported. The role of the tube-shaped structures in the formation and evolution of the barb is unclear. Please keep in mind that we only recently observed these structures and the exact direction of magnetic fields may not align with these structures because of the lack of vector magnetic field data. Even though the weather was not very good on 2013 September 29, the evolution of the barb can clearly be seen. However, the material flows in the filament threads of the filament were not observed.

To study the material flows in the filament, another quiescent filament on 2012 November 2 was examined. This quiescent filament was located close to the south pole. The center of the field of view was located at $x = -300''$ and $y = -743''$.

Figure 4 shows the high-resolution Hα image of the quiescent filament at 05:53:07 UT observed by NVST. The filament is composed of the threads in the spine. The angle between the spine and the threads is about 36 degrees. From the evolution of the filament, we found that the material flow in the filament threads is different from the results obtained by some previous researchers (Zirker et al. 1998; Lin et al. 2003). Zirker et al. (1998) and Lin et al. (2003) found steady bidirectional streaming everywhere in the filament along adjacent closely spaced threads. However, we found that the counter-streaming flows in this filament did not obey the rule that the flows in adjacent threads have opposite directions. The flows in one patch of the filament threads had the same direction but the flows in the adjacent patch of the filament threads had opposite directions. This finding is consistent with the large-scale counter-streaming flows in an EUV filament channel observed by Chen et al. (2014).

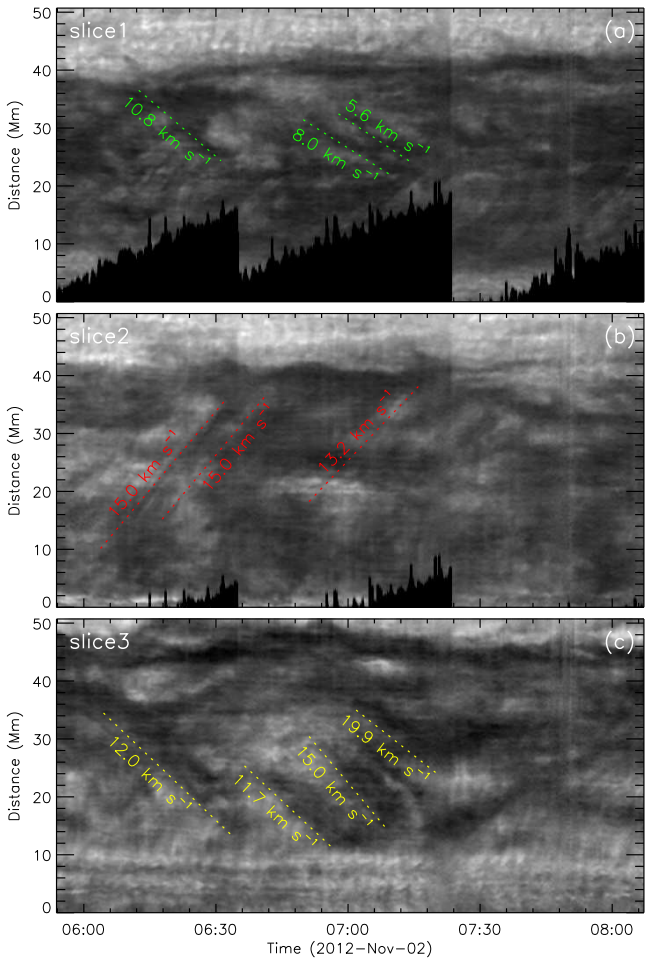

Fig. 5 The three time slices taken from high-resolution Hα images at positions marked by the numbered lines in Fig. 4. The velocities of the counter-streaming flows are marked in the figure.

To calculate the exact velocity of the material flows, we make one time slice every five pixels along the filament spine, which is parallel to the threads of the filament with an inclination angle of 36 degrees. In Figure 4, we selectively draw 12 lines with different colors every 20 pixels to show the different regions with material flows in opposite directions. Along the filament spine, we make 40 time slices between the uppermost yellow line and the lowermost green line in total to calculate the velocities of the material flows. Lin et al. (2009) found that the individual threads swayed back and forth sideways in the plane of the sky with quite a small amplitude (< 100 km). To eliminate the swaying motion of the threads, we take the average intensity of the three pixels perpendicular to the line, in which one pixel is on the line and the other two pixels are on both sides of the point. We found that there was large-scale counter-streaming with a certain range in the filament. Lines with the same color indicate that the material flows along these lines have the same direction. We give three examples to show how the material flows with time. Lines 1, 2 and 3 are parallel to the threads of the filament and are positioned over the threads. We make three time slices along these

three positions to show how the mass flows with time. Time slice 1, slice 2 and slice 3 along the three lines, marked by 1, 2 and 3 in Figure 4 respectively, are shown in Figure 5. We trace the features to estimate the velocity along the threads by using a linear fitting. The velocities of counter-streaming flows range from 5.6 km s^{-1} to 15.0 km s^{-1}. This process of evolution for the filament can be seen from supplementary movie 2 (*http://www.raa-journal.org/docs/Supp/ms1934movie2.avi*).

4 CONCLUSION AND DISCUSSION

The small-scale structures of filament barbs and counter-streaming flows in the threads were investigated in detail by using high resolution Hα data. First, we found that the thin threads in the barb can form parallel tube-shaped structures with a width of about 3 Mm. These structures formed during the evolution of the barb. Following the material flows from the spine to the barb, these structures merged and disappeared; Second, we found large-scale counter-streaming flows in a certain range along the threads in the filament spine rather than the steady bidirectional counter-streaming flows everywhere in the filament along adjacent closely spaced threads. The velocities of the counter-streaming flows range from 5.6 km s^{-1} to 15.0 km s^{-1}.

The thin dark threads along the quiescent filament spines and barbs have been observed by the Swedish 1-m Solar Telescope (SST) and Dutch Open Telescope (Heinzel 2007). These threads are regarded as the shear of the magnetic field lines. The flowing plasmas along the thin threads are considered to be evidence that alignment of the threads with the local magnetic field (Martin et al. 2008). Chae et al. (2005) suggested that filament barbs are cool matter suspended in local dips in the magnetic field lines formed by magnetic reconnection in the chromosphere. However, the detailed evolution of the barbs has not been investigated by previous authors. The barb investigated in this paper is a typical mature one. The boundary between the barb and the surrounding atmosphere is very neat. The threads of the barb are smoothly connected to the spine of the filament. Unlike the filaments studied by Lin et al. (2005, 2007), the parallel threads of the filament studied in this paper have an angle of about 36 degrees with respect to the spine of the filament. The parallel tube-shaped structures are formed during evolution of the barb, which has not been reported in a previous paper. The same phenomenon did not occur in the spine of the filament during its evolution. The width of these structures in the barb ranges from about 2.3 Mm to 3.3 Mm, which is larger than the width of the threads (150–450 km) obtained by Lin et al. (2005). The nature of these parallel structures deserves further investigation. Because the velocities of the flows in the vertical threads of the quiescent filaments are lower than their free-fall velocities, Chae et al. (2008) and Chae (2010) proposed magnetic dips in the initially horizontal magnetic fields to explain this phenomenon. We only observed downflow from the spine to the barb. As this filament was observed in the solar disk, the upflows in the vertical structures of the prominences found by Berger et al. (2010) cannot be observed. Joshi et al. (2013) found that the formation and disappearance of the filament barbs are closely related to the material flows. Our results also confirm this viewpoint. However, understanding why the parallel tube-shaped structures appear during the evolution of the barb and their role in the barb formation and evolution needs more observation and simulation.

The steady bidirectional streaming everywhere in the filament along adjacent closely spaced threads was discovered by Zirker et al. (1998). They found that the counter-streaming is especially clear in the spine, but the same phenomenon also exists in the barbs. Therefore, the counter-streaming flows are also claimed to exist in the filament by several authors (Lin et al. 2003; Schmieder et al. 2008). Ahn et al. (2010) found that the pattern of horizontal counter-streaming motions is due to the return of the moving plasma fragments. However, from our observation, we have not found the ubiquitous Hα counter-streaming flows in adjacent threads of the filament that were reported by previous researches (Zirker et al. 1998; Lin et al. 2003; Schmieder et al. 2008). We found that the large-scale counter-streaming flows existed in the filament spine. One patch of the flows showed the same direction and an adjacent patch of the flows displayed opposite directions. The width of the patches was

about $10''$. The patches exhibited alternating directions along the spine of the filament. This result is different from that of Zirker et al. (1998). Chen et al. (2014) used the extreme ultraviolet (EUV) spectral observations and found there are no EUV counterparts of the Hα counter-streaming flows in the filament channel. The larger-scale patchy counter-streaming flows in EUV along the filament channel were found from one polarity to the other (Chen et al. 2014). The upflows and downflows observed by Chen et al. (2014) were about 10 km s^{-1}, which are the same as the transverse velocities along the filament threads obtained by us. They suggested that the ubiquitous Hα counter-streaming flows found by previous researchers are due to the longitudinal oscillations of the filament threads, which are not in phase with each other. The results mentioned above are obtained by using the line-of-sight velocity or Doppler velocity and they have not traced the transverse motion of the features of the filament observed by Hα observation.

From our observation, we found that the dark material flows are co-aligned well with the threads and do not cross the threads. Moreover, our results show that there is a large-scale counter-streaming flow with a certain range in the threads of the quiescent filament. Ubiquitous Hα counter-streaming flows in adjacent threads of the filament are not found in our example. The long oscillation period of a quiescent filament is 98 minutes, as obtained by Ning et al. (2009a). The continuous material flows along the threads lasted for about two hours and fourteen minutes and did not change their directions during our observation. If the material flows are caused by the transverse oscillation of the filament, we should have observed the returning flows. Lin et al. (2009) and Lin (2011) found that the period of the swaying motions of individual filament threads is about 5 minutes by using high-resolution observations obtained by the SST in La Palma. The same period was also obtained by Ning et al. (2009b) by analyzing small-scale oscillations in a quiescent prominence observed by Hinode. Parenti (2014) presented a detailed review of the oscillation of the prominences. Moreover, the amplitude of the transverse oscillation was very small, about 5 Mm (Ning et al. 2009b). The continuous material flows can last for the whole observational time and did not change their direction. Therefore, we think that these flows are not caused by the transverse oscillation of the filament. Our result supports the viewpoint suggested by Chen et al. (2014) and Okamoto et al. (2007) that ubiquitous Hα counter-streaming flows in adjacent threads of the filament may be driven by the longitudinal oscillation of the filament threads. Berger et al. (2010) found that plasma forming the prominence is entrained by the upflows, which have ascent speeds of 13–17 km s^{-1}. The fine structures acquired at Ca II H have a rising speed of 5–20 km s^{-1} before the formation of the filament (Okamoto et al. 2010). Some of them fell down after reaching their maximum heights, while others rose with decelerating speed and stayed in the corona. The upflows may be counterbalanced by ubiquitous downflows in the prominence (Berger et al. 2008). The detailed relationship between the downflow/upflow and the transverse material flows in the threads of the quiescent filament deserves further investigation.

Acknowledgements The authors are grateful to the referee for his/her constructive suggestions. This work is supported by the National Natural Science Foundation of China (NSFC) under grant numbers 11373066, 11373065 and 11203077, the Yunnan Science Foundation of China under number 2013FB086, the Talent Project of Western Light of Chinese Academy of Sciences, the National Basic Research Program of China (973 program) under grant number G2011CB811400, and the Key Laboratory of Solar Activity of CAS under number KLSA 201303, KLSA 201412 and KLSA 201407. The authors thank Rui Wang and Dingchang Wang for their observations. Youth Innovation Promotion Association of CAS (No. 2011056)

References

Ahn, K., Chae, J., Cao, W., & Goode, P. R. 2010, ApJ, 721, 74
Aulanier, G., & Demoulin, P. 1998, A&A, 329, 1125
Berger, T. E., Shine, R. A., Slater, G. L., et al. 2008, ApJ, 676, L89
Berger, T. E., Slater, G., Hurlburt, N., et al. 2010, ApJ, 716, 1288

Cao, W., Ning, Z., Goode, P. R., Yurchyshyn, V., & Ji, H. 2010, ApJ, 719, L95
Chae, J. 2010, ApJ, 714, 618
Chae, J., Ahn, K., Lim, E.-K., Choe, G. S., & Sakurai, T. 2008, ApJ, 689, L73
Chae, J., Moon, Y.-J., & Park, Y.-D. 2005, ApJ, 626, 574
Chen, P. F., Harra, L. K., & Fang, C. 2014, ApJ, 784, 50
Engvold, O. 1998, in Astronomical Society of the Pacific Conference Series, 150, IAU Colloq. 167: New Perspectives on Solar Prominences, eds. D. F. Webb, B. Schmieder, & D. M. Rust, 23
Engvold, O., Jakobsson, H., Tandberg-Hanssen, E., Gurman, J. B., & Moses, D. 2001, Sol. Phys., 202, 293
Fang, C., Chen, P.-F., Li, Z., et al. 2013, RAA (Research in Astronomy and Astrophysics), 13, 1509
Feng, S., Deng, L., Shu, G., Wang, F., Deng, H., Ji, K. 2012, In Advanced Computational Intelligence (ICACI), IEEE Fifth International Conference on, 626
Gao, G., Wang, M., Dong, L., Wu, N., & Lin, J. 2014, New Astron., 30, 68
Heinzel, P. 2007, in Astronomical Society of the Pacific Conference Series, 368, The Physics of Chromospheric Plasmas, eds. P. Heinzel, I. Dorotovič, & R. J. Rutten, 271
Hirayama, T. 1985, Sol. Phys., 100, 415
Joshi, A. D., Srivastava, N., Mathew, S. K., & Martin, S. F. 2013, Sol. Phys., 288, 191
Kong, D., Xiang, N., & Pan, G. 2014, PASJ, 66, 28
Kong, D.-F., Qu, Z.-N., & Guo, Q.-L. 2015, RAA (Research in Astronomy and Astrophysics), 15, 77
Li, K.-J., Liang, H.-F., & Feng, W. 2010, RAA (Research in Astronomy and Astrophysics), 10, 1177
Li, L., & Zhang, J. 2013, Sol. Phys., 282, 147
Lin, Y. 2011, Space Sci. Rev., 158, 237
Lin, Y., Engvold, O. R., & Wiik, J. E. 2003, Sol. Phys., 216, 109
Lin, Y., Engvold, O., Rouppe van der Voort, L., Wiik, J. E., & Berger, T. E. 2005, Sol. Phys., 226, 239
Lin, Y., Engvold, O., Rouppe van der Voort, L. H. M., & van Noort, M. 2007, Sol. Phys., 246, 65
Lin, Y., Soler, R., Engvold, O., et al. 2009, ApJ, 704, 870
Liu, Z., Qiu, Y., & Lu, R. 1998, in Society of Photo-Optical Instrumentation Engineers (SPIE) Conference Series, 3561, Electronic Imaging and Multimedia Systems II, eds. L. Zhou, & C.-S. Li, 326
Liu, Z., Xu, J., Gu, B.-Z., et al. 2014, RAA (Research in Astronomy and Astrophysics), 14, 705
Lohmann, A. W., Weigelt, G., & Wirnitzer, B. 1983, Appl. Opt., 22, 4028
Mackay, D. H., Karpen, J. T., Ballester, J. L., Schmieder, B., & Aulanier, G. 2010, Space Sci. Rev., 151, 333
Martin, S. F. 1998, Sol. Phys., 182, 107
Martin, S. F., Lin, Y., & Engvold, O. 2008, Sol. Phys., 250, 31
Ning, Z., Cao, W., & Goode, P. R. 2009a, ApJ, 707, 1124
Ning, Z., Cao, W., Okamoto, T. J., Ichimoto, K., & Qu, Z. Q. 2009b, A&A, 499, 595
Okamoto, T. J., Tsuneta, S., Berger, T. E., et al. 2007, Science, 318, 1577
Okamoto, T. J., Tsuneta, S., & Berger, T. E. 2010, ApJ, 719, 583
Parenti, S. 2014, Living Reviews in Solar Physics, 11, 1
Schmieder, B., Bommier, V., Kitai, R., et al. 2008, Sol. Phys., 247, 321
Tandberg-Hanssen, E., ed. 1995, Astrophysics and Space Science Library, 199, The Nature of Solar Prominences, 91
Tubbs, R. N. 2004, The Observatory, 124, 159
van Ballegooijen, A. A. 2004, ApJ, 612, 519
Wang, R., Xu, Z., Jin, Z.-Y., et al. 2013, RAA (Research in Astronomy and Astrophysics), 13, 1240
Weigelt, G. P. 1977, Optics Communications, 21, 55
Yang, Y.-F., Qu, H.-X., Ji, K.-F., et al. 2014, arXiv:1407.7958
Zhou, Y.-H., Chen, P.-F., Zhang, Q.-M., & Fang, C. 2014, RAA (Research in Astronomy and Astrophysics), 14, 581
Zirker, J. B., Engvold, O., & Martin, S. F. 1998, Nature, 396, 440